JACS
JOURNAL OF THE AMERICAN CHEMICAL SOCIETY
Article
pubs.acs.org/JACS

A Resistance-Switchable and Ferroelectric Metal–Organic Framework

Liang Pan,[†,∥,∇] Gang Liu,[†,∥,∇] Hui Li,[‡] Sheng Meng,[‡] Lei Han,*[,§] Jie Shang,[†,∥] Bin Chen,[†,∥] Ana E. Platero-Prats,[⊥] Wei Lu,[#] Xiaodong Zou,*[,⊥] and Run-Wei Li*[,†,∥]

[†]Key Laboratory of Magnetic Materials and Devices, Ningbo Institute of Materials Technology and Engineering, Chinese Academy of Sciences, Ningbo, Zhejiang 315201, China

[‡]Institute of Physics, Chinese Academy of Sciences, Beijing 100190, China

[§]State Key Laboratory Base of Novel Functional Materials and Preparation Science, School of Materials Science and Chemical Engineering, Ningbo University, Ningbo, Zhejiang 315211, China

[∥]Zhejiang Province Key Laboratory of Magnetic Materials and Application Technology, Ningbo Institute of Materials Technology and Engineering, Chinese Academy of Sciences, Ningbo, Zhejiang 315201, China

[⊥]Inorganic and Structural Chemistry and Berzelii Centre EXSELENT on Porous Materials, Department of Materials and Environmental Chemistry, Stockholm University, SE-106 91 Stockholm, Sweden

[#]Department of Electrical Engineering and Computer Science, University of Michigan, Ann Arbor, Michigan 48109-2122, United States

Supporting Information

ABSTRACT: The ever-emerging demands on miniaturization of electronic devices have pushed the development of innovative materials with desired properties. One major endeavor is the development of organic- or organic–inorganic hybrid-based electronics as alternatives or supplements to silicon-based devices. Herein we report the first observation of the coexistence of resistance switching and ferroelectricity in a metal–organic framework (MOF) material, $[InC_{16}H_{11}N_2O_8]\cdot 1.5H_2O$, denoted as **RSMOF-1**. The electrical resistance of **RSMOF-1** can be turned on and off repeatedly with a current ratio of 30. A first-principles molecular dynamics simulation suggests that the resistive switching effect is related to the ferroelectric transition of N···H–O···H–N bridge-structured dipoles of the guest water molecules and the amino-tethered MOF nanochannel. The discovery of the resistive switching effect and ferroelectricity in MOFs offers great potential for the physical implementation of novel electronics for next-generation digital processing and communication.

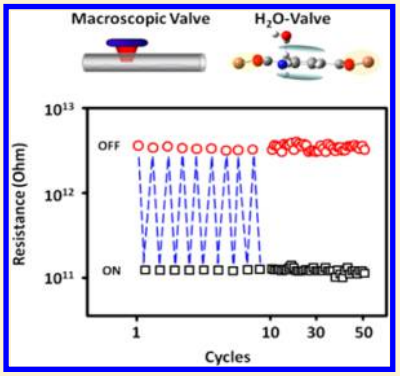

INTRODUCTION

Designing novel device concepts and discovering new functionalities are among the major tasks for materials scientists. To match the continuous development of global IT industries and the device-shrinking campaign in the post-Moore era, organic and hybrid electronics are of great importance and require the rational design and synthesis of functional materials with desired and controllable electronic properties.[1−4] Among the various candidates of molecules and ensembles of molecules,[5−9] metal–organic frameworks (MOFs) are a unique class of hybrid crystalline materials that are distinguished by great chemical versatility, an extraordinary degree of variability, and three-dimensional periodicity in their functionalities.[10−12] More importantly, because they are formed by the assembly of metal cations/clusters ("nodes") and multitopic organic bridging ligands ("linkers"), deliberate tuning of the optical, ferroelectric, magnetic, and multiferroic properties of MOFs is possible by means of the synergistic interplay between the organic linkers and metal nodes as well as the host–guest interactions between sorbed guest molecules and the solid framework, leading to huge possibilities in optoelectronic and spintronic device applications.[13−15]

Nevertheless, toward the physical implementation of MOF-based electronic applications, it is still an appealing challenge to characterize, understand, and modulate the charge transport properties of such organic-and-inorganic integrated systems.[16,17] In this contribution, we report the first observation of resistive and ferroelectric switching behaviors in an indium MOF material, denoted as **RSMOF-1** (RSMOF = resistance-switchable metal–organic framework), with the chemical formula $[InC_{16}H_{11}N_2O_8]\cdot 1.5H_2O$ and a twofold-interpenetrated three-dimensional (3D) β-quartz topology (Figure 1 and Figure S1 in the Supporting Information). The resistive and ferroelectric switching behaviors of **RSMOF-1** occur at room temperature with excellent reproducibility and low power consumption characteristics that are important for electronic device applications. Experimental observations and a molecular

Received: August 20, 2014
Published: November 24, 2014

   dx.doi.org/10.1021/ja508592f | J. Am. Chem. Soc. 2014, 136, 17477−17483

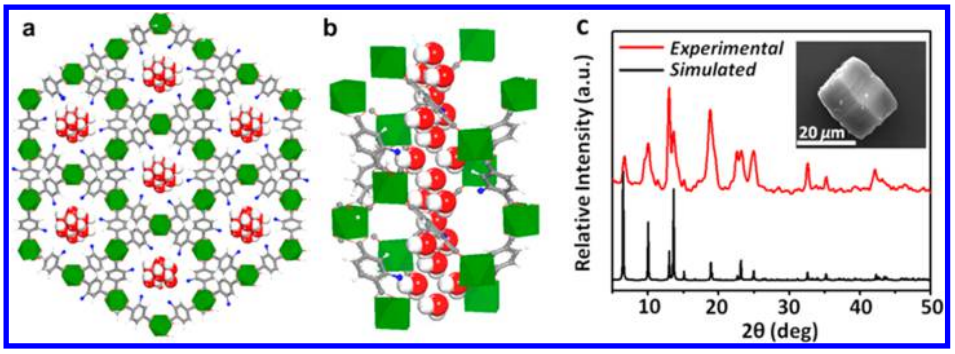

Figure 1. Crystal structure and X-ray diffraction patterns of **RSMOF-1**. (a, b) The structure obtained by single-crystal X-ray diffraction viewed (a) along the *c* axis and (b) along the *b* axis. Water molecules are located in the nanochannels. Amino groups and one symmetry-independent water molecule are disordered in four positions, and only one of them is shown. Because of the disorder, hydrogen atoms were not located. However, they have been added for a better illustration of the structure. InO_8 polyhedra are shown in green. (c) Experimental (red) and simulated (black) powder X-ray diffraction patterns of **RSMOF-1**. The inset shown a scanning electron microscopy image of an **RSMOF-1** single crystal.

dynamics simulation suggest that the resistive and ferroelectric switching properties are strongly regulated by the presence of guest water molecules in the nanochannels through electric-field-controlled hydrogen-bonding interactions with the amino-tethered **RSMOF-1**.

METHODS

Synthesis and Characterization. A mixture of indium nitrate monohydrate ($In(NO_3)_3{\cdot}H_2O$) (61.4 mg), 2-amino-1,4-benzenedicarboxylic acid (NH_2-BDC) (77.1 mg), and 1,4-diazabicylo[2.2.2]octane (DABCO) (20.0 mg) was stirred vigorously in *N*,*N*-dimethylformamide (DMF) (5.0 g) for 30 min to give a homogeneous solution. The reaction mixture was then sealed in a Teflon-lined stainless steel autoclave and heated at 120 °C for 3 days. After being cooled to room temperature, the resulting colorless crystals of **RSMOF-1** were collected and thoroughly washed with DMF. The morphology of the crystals is hexagonal prismatic (Figure S2), which is consistent with the point group of **RSMOF-1** with the *c* axis perpendicular to the hexagonal planes.[18] The calculated yield was ∼70%. Fourier transform infrared data (KBr 4000−400 cm^{-1}, spectrum shown in Figure S3): 3450, 3363, 3200, 2955, 2930, 1660, 1623, 1566, 1500, 1433, 1384, 1257, 1153, 1100, 866, 835, 769, 584, 526. All chemicals and solvents were purchased from Sigma-Aldrich and used as received.

Single-Crystal Structure Determination. Single-crystal X-ray diffraction data of the as-synthesized **RSMOF-1** were recorded at room temperature on an Oxford Diffraction Xcalibur 3 diffractometer with Mo Kα radiation (λ = 0.71073 Å). Data reduction and empirical absorption correction were performed using CrysAlisPro. The structures were solved and refined using SHELXS-97.[19] All non-hydrogen atoms could be located directly from the difference Fourier maps. Each N atom is disordered in four possible positions with occupancies of 0.25. One of the water positions is partially occupied with occupancy of 0.25. Therefore, the hydrogen atoms were not added in the CIF file. The crystal data and structure refinement details are given in Table S1 in the Supporting Information. CCDC no. 944730 contains the supplementary crystallographic data for **RSMOF-1**. These data can be obtained free of charge at www.ccdc.cam.ac.uk/conts/retrieving.html; from the Cambridge Crystallographic Data Centre, 12 Union Road, Cambridge CB2 1EZ, U.K.; or by e-mail at deposit@ccdc.cam.ac.uk.

Fabrication and Measurements. The Pt/Ti/SiO_2/Si substrates were precleaned sequentially with ethanol, acetone, and isopropanol in an ultrasonic bath, each for 20 min. A single crystal of **RSMOF-1** with approximate dimensions of 10 μm (*a*) × 10 μm (*b*) × 20 μm (*c*) was selected and bonded along the *c* axis onto the substrate using silver conducting glue. A tungsten tip with a diameter of 250 nm was in direct contact with the hexagonal plane of the crystal and served as the top electrode. The transport properties of the single crystal were evaluated through direct current (dc) current−voltage (*I*−*V*) characteristic measurements on a Lakeshore probe station at various temperatures and recorded by a Keithley 4200 semiconductor characterization system in voltage-sweeping mode. The sensitivity of the Keithley 4200 system was 10 fA. During the *I*−*V* measurements, a bias voltage was applied through the tungsten tip with a sweeping step of 0.01 V, while the platinum substrate was always grounded. A compliance current (CC) preset of 5.0×10^{-11} A was used to avoid overstriking or permanent breakdown of the sample. The evaluation of the ON/OFF operation of the single crystal was conducted in a similar way. The alternating current (ac) conductivity of the sample was also evaluated using a Solartron 1260A impedance analyzer. Temperature-dependent polarization−electric field (*P*−*E*) loops were measured on the same single crystal using a ferroelectric testing system (Precision Premier II, Radiant Technologies) with 0.2 Hz to 2 MHz triangular-waveform ac electrical fields applied along the *c* axis of the crystal. The frequency-dependent dielectric constant−temperature (ε−*T*) characteristics of the single crystal were measured on a Tonghui TH2828A impedance analyzer over the frequency range from 1 kHz to 1 MHz at a heating/cooling rate of 5 K/min.

Ab Initio Molecular Dynamics Simulation. A first-principles Born−Oppenheimer molecular dynamics (BOMD) simulation based on density functional theory (DFT) in the Perdew−Burke−Ernzerhof (PBE) framework using the CP2K code was performed to investigate the structural and dynamical properties of the water molecules trapped in the nanochannels of **RSMOF-1**.[20−22] A mixed Gaussian and plane-wave (GPW) basis set was used, with the Goedecker−Teter−Hutter (GTH) pseudopotential to describe the interaction between valence electrons and atomic cores.[23,24] The Grimme dispersion correction was also employed to better describe the hydrogen-bonding interactions between water molecules and amino groups.[25] The MD simulation was performed in the constant-volume (*NVT*) ensemble at 300 K. To simplify the simulation and provide a better illustration of the dynamics of the water molecules involved in the single crystal, the amino groups were placed at one of the equivalent positions. Initially, the water molecules were placed equidistantly in the center of the nanochannel, while the protons were allowed to be attached randomly to either water or an amino group in the simulation cell. A time step of 1.0 fs was selected, and the entire simulation covered 20 ps. The dipole moments of guest water molecules were estimated using the structure obtained from the MD trajectory and the atomic charges in the three-site SPC water model, in which the charges of O and H atoms are fixed at −0.82*e* and 0.41*e*, respectively.

RESULTS AND DISCUSSION

Colorless hexagonal prismatic crystals of **RSMOF-1** (Figure S2) were synthesized through a solvothermal route. **RSMOF-1** crystallizes in the chiral hexagonal space group $P6_222$ with *a* = 15.683(3) Å and *c* = 11.5526(16) Å (Table S1). The asymmetric unit contains an indium atom, two NH_2-BDC

dx.doi.org/10.1021/ja508592f | J. Am. Chem. Soc. 2014, 136, 17477−17483

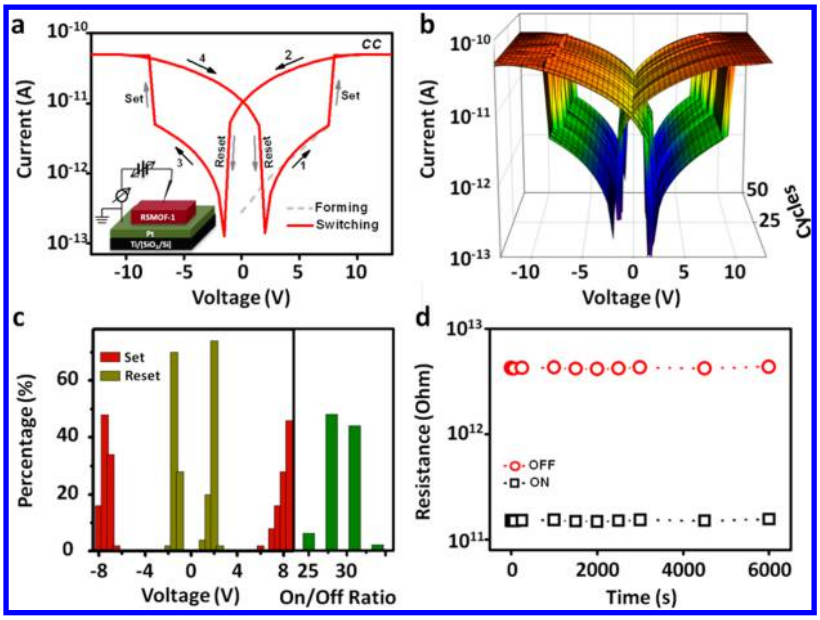

Figure 2. Resistive switching properties of **RSMOF-1**. (a) Semilogarithmic plot of the room-temperature current−voltage (I−V) characteristics of the single crystal. The arrows indicate the sweeping direction while the numbers represent the sweeping sequence. CC stands for the compliance current (5.0×10^{-11} A). The inset shows a schematic illustration of the sample configuration for the I−V measurements. (b) I−V curves and (c) distribution of the set/reset voltages and the ON/OFF ratio for 50 consecutive cycles. (d) Retention performance of the two conductance states over 6000 s. The resistance of the sample was read at 0.1 V.

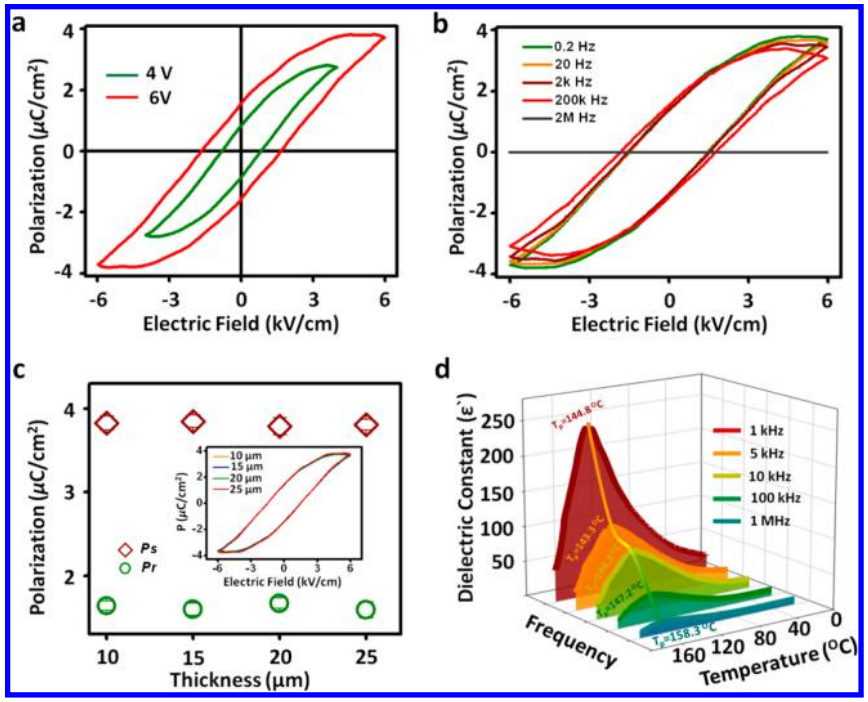

Figure 3. Ferroelectric properties of **RSMOF-1**. (a) Room-temperature polarization−electric field (P−E) characteristics of the single crystal recorded under maximum voltages of ±6 V and ±4 V. (b) Frequency-dependent and (c) sample-thickness-independent ferroelectric polarization of the single crystal of **RSMOF-1** recorded between +6 V and −6 V. (d) Frequency-dependent dielectric constant−temperature (ε−T) characteristics of the single crystal as measured from 1 kHz to 1 MHz.

linkers, and 1.5 guest water molecules. Each indium atom is coordinated to four NH_2-BDC ligands through eight oxygen atoms from four carboxylate groups to form an InO_8 polyhedron. The lengths of the In−O chelating bonds range from 2.250(8) to 2.271(10) Å. Each InO_8 polyhedron is connected to four other InO_8 polyhedra via the linear NH_2-BDC ligands, forming a twofold-interpenetrated 3D anionic coordination network with the β-quartz topology (Figure S1). Extra protons reside on the amino and carboxylate groups to neutralize the framework (Figure S3 and Movie S1), while guest water molecules are trapped in the hexagonal helical nanochannels of the MOF material with an amine-functionalized wall running in the c direction (Figure 1). The water molecules in the channel form a hydrogen-bonding network.

dx.doi.org/10.1021/ja508592f | J. Am. Chem. Soc. 2014, 136, 17477−17483

The diameter of the nanochannel is 7.4 Å. The total solvent-accessible volume of **RSMOF-1** is 1310.9 Å^3, as calculated using PLATON,[26] and corresponds to ca. 53.3% of the unit cell volume (2460.8 Å^3). The geometric parameters in the coordination sphere of **RSMOF-1** are similar to those of its analogues.[27−30] The phase purity of **RSMOF-1** was confirmed by powder X-ray diffraction, as shown in Figure 1c. Thermogravimetric analysis (TGA) in a nitrogen flow revealed that **RSMOF-1** is stable up to 160 °C (Figure S4).

RSMOF-1 demonstrates symmetric and bipolar resistive switching behavior at room temperature, as shown by its dc current−voltage (I−V) characteristics (Figure 2a). The sweeping bias voltage was applied along the c axis of the single crystal, and a forming process was always needed before testing. An Ohmic contact was established between the electrode and the single crystal, and the I−V characteristics demonstrated a linear nature, as shown in Figure S5. The frequency- and temperature-dependent ac conductivity of the MOF crystal is shown in Figure S6. The dc conductivity obtained by extrapolation of the plateau of the σ−f curve to the low-frequency end is comparable to that calculated from Figure S5.[31] When the voltage was swept in the direction of 0 V → 13 V → 0 V → −13 V → 0 V, **RSMOF-1** was switched continuously between two resistance states with uniformly distributed threshold voltages of about ±7.5 V (set) and ±1.5 V (reset) and a stable ON/OFF ratio of ∼30 (read at ±2.5 V) (Figure 2b,c). Both states can be retained for at least 6000 s (Figure 2d), which indicates that the observed resistive switching in **RSMOF-1** is nonvolatile. It is noteworthy that the I−V characteristics of **RSMOF-1** exhibit exotic nonzero-voltage minima upon being reset, which may be ascribed to the electrochemical process associated with the use of the redox-active silver conducting glue in fabrication of the device[32] or the inertial ionic conduction when the external electrical field was decreased to zero.

Interestingly, as shown in the polarization−electric field (P−E) characteristics (Figure 3a), **RSMOF-1** demonstrates polarization switching behavior with a saturation polarization (P_s) of ∼3.81 μC/cm^2, a remnant polarization (P_r) of 1.64 μC/cm^2, and a coercive field (E_c) of 1.65 kV/cm when the potential is scanned between ±6 V along the c axis. When the applied voltage maximum is decreased from ±6 to ±4 V, both the saturated and remnant polarizations as well as the coercive field decrease accordingly. With a decrease in the frequency of the ac electric field applied to the single crystal, the saturated polarization of the P−E loops increases while the coercivity decreases accordingly (Figure 3b). The polarization of **RSMOF-1** also shows thickness-independent characteristics (Figure 3c). Moreover, the dielectric constant−temperature (ε−T) characteristics exhibit a frequency-dependent broad band over the wide temperature range from 17 to 183 °C (Figure 3d), wherein the dielectric constant maxima correspond to the order−disorder (or paraelectric−ferroelectric) transition of a ferroelectric material. Such a transition cannot be observed in electrets or leaky dielectrics, therefore suggesting that the single crystal of **RSMOF-1** is ferroelectric in nature. Similar ferroelectricity has also been demonstrated in other systems containing guest water molecules in porous materials and is ascribed to the alignment of the hydrogen-bonding-related dipoles (see detailed discussion below).[33] As the frequency is increased from 1 kHz to 1 MHz, the dielectric constant maximum decreases from 243 to 16 while the transition temperature shifts from 130 to 160 °C, thus implying that **RSMOF-1** behaves as a relaxor ferroelectric.[34−36]

It is noteworthy that the $P6_222$ space group of the framework inevitably leads to a nonpolar compound,[37,38] and therefore, the ferroelectricity of **RSMOF-1** might be correlated to the incorporation of guest water molecules in the nanochannels.[33a,39] The presence of amino groups in the channels provides abundant sorption sites for water molecules through hydrogen-bonding interactions.[40−42] Changing the sample temperature can disturb the hydrogen-bonding interactions non-negligibly, partially remove the guest water molecules (Figure S7), and thus may influence the ferroelectric properties of **RSMOF-1** significantly. As shown in Figure 4a, the P−E loops of **RSMOF-1** shrink and eventually disappear as the temperature rises from

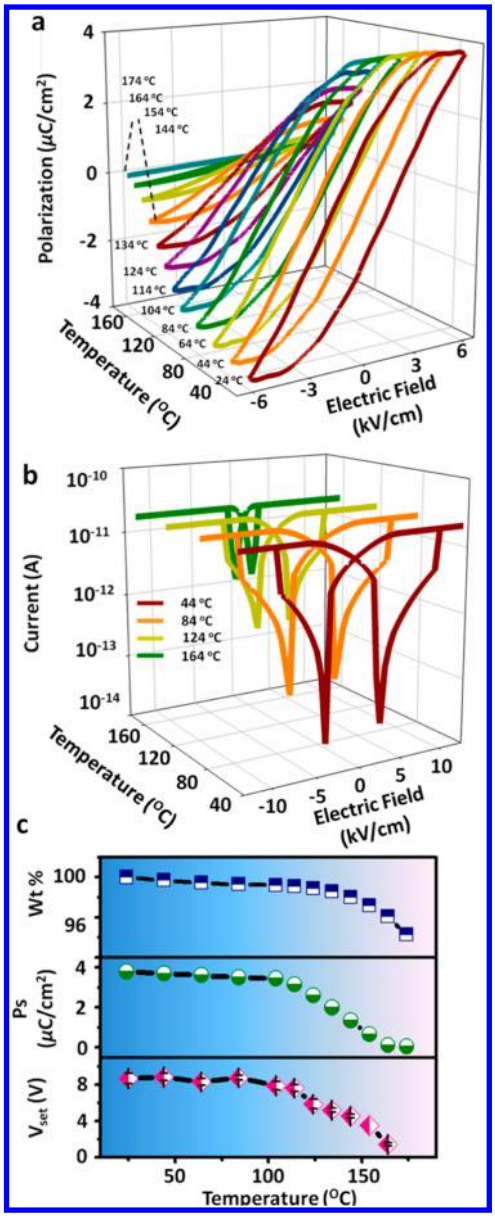

Figure 4. (a, b) Temperature-dependent (a) polarization−electric field and (b) current−electric field characteristics of the **RSMOF-1** single crystal recorded over the temperature range from 24 to 164 °C. (c) Weight percent−temperature (wt %−T, derived from TGA results), saturation polarization−temperature (P_s−T), and set voltage−temperature (V_{set}−T) relationships of the single crystal.

dx.doi.org/10.1021/ja508592f | J. Am. Chem. Soc. 2014, 136, 17477−17483

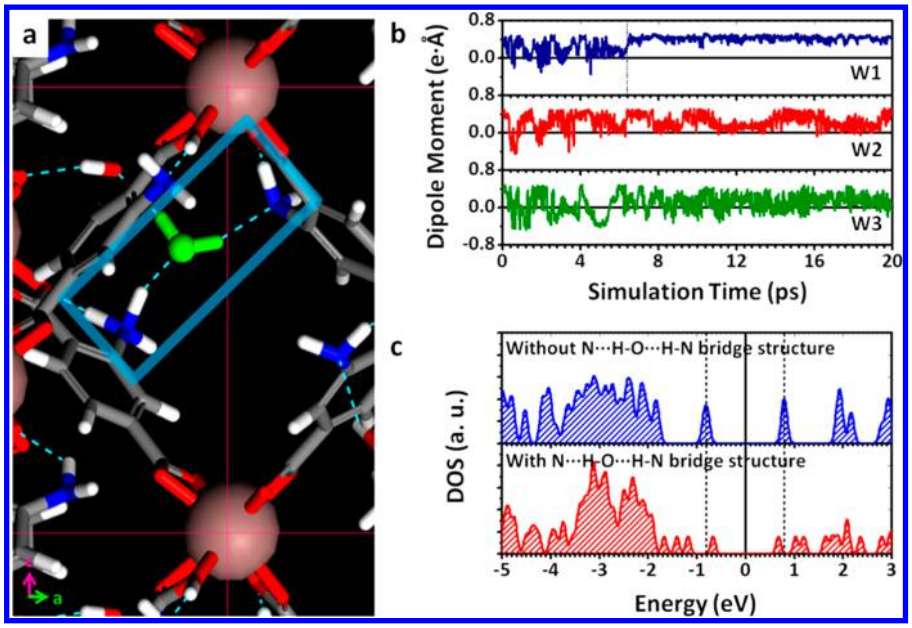

Figure 5. Guest–host interactions between water molecules and amino groups in the **RSMOF-1** crystal nanochannel and its influence on the electronic structure of **RSMOF-1**. (a) Snapshot of the spontaneous formation of the stable N···H–O···H–N bridge structure. The MD simulation was conducted at 300 K and lasted for 20 ps. The water molecule with the stable hydrogen bonds is highlighted in green. Color code: In, pink; N, blue; O, red; H, white. (b) Time-resolved dipole moment evolution of the water molecules trapped in the nanochannel of **RSMOF-1**. The blue curve corresponds to the dipole moment of the N···H–O···H–N bridge structure formed with water molecule W1, while the red and green curves correspond to the dipole moments of water molecules forming weak and intermittent hydrogen-bonding interactions. (c) Local density of states (DOS) of **RSMOF-1** calculated before and after the formation of the stable ice-like N···H–O···H–N bridge structure.

24 to 174 °C. Similar to the ferroelectric characteristics under different temperatures, the resistive switching properties of **RSMOF-1** also strongly depend on the sample temperature (Figure 4b). As the sample temperature is increased from 24 to 164 °C, the *I*–*V* loops shrink with decreases in both the threshold voltages and the ON/OFF ratio. Once the sample temperature reaches 174 °C, the resistive switching behavior vanishes. Furthermore, both the saturation polarization–temperature (P_s–T) and set voltage–temperature (V_{set}–T) relationships follow the weight percent–temperature (wt %–T) trend of the TGA results (Figure 4c), again suggesting that the sorbed guest water molecules play a key role in the resistive switching and ferroelectricity of **RSMOF-1**.

To reveal the dynamic behavior of the water molecules and the possible effect of hydrogen bonds on the electronic structures as well as the microscopic origin of the ferroelectricity, a first-principles MD simulation was performed to investigate the dynamical interaction between the guest water molecules and the **RSMOF-1** framework (Figure 5a). To simplify the simulation, all of the amino groups were placed at the same equivalent position of the NH_2-BDC linkers along the *c* direction, while the water molecules were initially placed equidistantly in the center of the **RSMOF-1** channel and allowed to stabilize spontaneously. During the 20 ps electric-field-free MD simulation, an N···H–O···H–N bridge structure is formed spontaneously after ca. 6 ps under ambient conditions, with one of the water molecules (displayed in green in Figure 5a and denoted as W1 in Figure 5b) moving toward the framework and interacting with neutral $-NH_2$ and charged $-NH_3^+$ amino groups. This bridged hydrogen-bonding structure remains stable until the end of the simulation, generating a constant dipole moment of 0.4 *e* Å along the *c* direction and an O_w···N distance of ∼2.9 Å (Figure 5b and Movies S1 and S2). Such a bridgelike strucure has an energy-degenerate counterpart with a net dipole moment in the opposite direction. Thus, it is reasonable that without effective regulation by external electric fields, the formation of N···H–O···H–N bridge structures will occur in random directions and **RSMOF-1** will be nonpolar in nature. However, an external electric field may force the N···H–O···H–N bridge structure to flip and get aligned along the external field direction, resulting in an order–disorder-type ferroelectric polarization of **RSMOF-1**. Although other water molecules also form hydrogen bonds with amino groups or water molecules intermittently, such hydrogen-bonding interactions are less stable compared with the aforementioned bridged hydrogen-bonding structure, and therefore, these water molecules exhibit dipole moments varying between ±0.4 *e* Å and can itinerate more freely inside the entire channel space, as shown by W2 and W3 in Figure 5b and Movie S1.

In MOFs, the carboxylate oxygen atoms, which glue the metal ions/clusters and organic linkers through σ bonds, meanwhile prevent the effective overlap of the π orbitals in the linkers with the metal d orbitals.[43,44] As a result, most MOFs are electrical insulators. Both metal-to-metal and linker-to-linker charge carrier hopping processes, which are less efficient compared with the charge carrier transport through conjugated systems, have been documented to dominate the electron transport behaviors of MOF materials.[45,46] On the other hand, it has been demonstrated that the formation of hydrogen bonds between the water molecules and the solid framework can effectively tune the electronic structure of **RSMOF-1**, leading to a rigid band gap decrease of 0.18 eV (Figure 5c). Both the density of states (DOS) and the DOS maxima on either side of the Fermi surface are influenced as well. Along with the electric-field-induced swing and flip of the N···H–O···H–N bridge structure, continuous modulation of the band gap, DOS, and DOS maxima via polarization-related atomic displacement and

dx.doi.org/10.1021/ja508592f | J. Am. Chem. Soc. 2014, 136, 17477–17483

symmetry distortion thus may strongly influence charge carrier hopping among the organic linkers.[47,48] Consequently, a decrease of 0.16 eV in the activation energy of the charge carrier hopping process is observed upon the occurrence of polarization switching in **RSMOF-1** (Figure S8).[49] When the majority of the bridging hydrogen bonds are aligned in the *c* direction, resistance switching from the initial high-resistance state to the low-resistance state occurs. Since the ferroelectric polarization can be switched reversibly, **RSMOF-1** can correspondingly undergo a reverse transition from the low-resistance state to the high-resistance state. Therefore, the forming−resetting−setting−resetting cycles of a resistive switching process can be completed by the water-molecule-related ferroelectric transition, which acts as a molecular valve to control the transport of charge carriers along the **RSMOF-1** framework. Certainly, other physicochemical effects, including the interfacial behavior in ferroelectrics (e.g., lowering of the Schottky barrier at the MOF−electrode interfaces due to polarization charge),[50] electric-induced pyrolysis of the organic linkers,[51] charge transfer between the organic linkers and the metal species,[52] and conformational changes of the framework,[53] may also contribute to the resistive switching of **RSMOF-1**.

Mimicking a macroscopic mechanical valve (Figure 6a), the role of water molecules acting as a control element to regulate the electron transport in **RSMOF-1** was further evaluated by the cyclic *I*−*V* switching behavior. As illustrated in Figure 6b, the resistance of **RSMOF-1** can be turned ON and OFF repeatedly under ambient conditions. With increasing sample temperature, the effective number of water molecules decreases significantly, which leads to a solid modulation of the OFF-state resistance and a gradual tuning (decrease) of the ON/OFF ratio in **RSMOF-1** (Figure S9). Upon integration of the set/reset voltage with the current readout at the corresponding ON/OFF transition point, a power consumption of ∼0.4 nW or 0.2 pW can be derived for the room-temperature "OPEN" or "CLOSE" operation of the **RSMOF-1** single-crystal-based electronic valves.

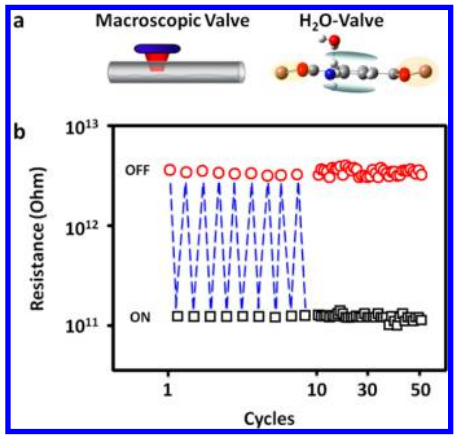

Figure 6. (a) Schematic illustration of the water molecule acting as a control element to regulate the electron transport of the solid RSMOF-1 framework. (b) Repeated resistance ON/OFF operation of RSMOF-1.

CONCLUSION

RSMOF-1 demonstrates resistive switching effect as well as ferroelectricity at room temperature with excellent reproducibility and low power consumption feature. Experimental observations and a molecular dynamics simulation showed that the electrical properties of **RSMOF-1** are strongly regulated by the guest water molecules through electric-field-controlled hydrogen-bonding interactions with the amine-tethered nanochannels. MOFs have not historically played a prominent role in electronic applications. However, the discovery of the resistive switching and ferroelectric behaviors in a MOF material as well as the improvements in our understanding and control of how MOFs transport charge and interact with the macroscopic world are bridging the gap between these fascinating materials and new devices and applications.

ASSOCIATED CONTENT

Supporting Information

Detailed information regarding instrumentation, crystal data (CIF) and structure refinement for **RSMOF-1**, and supporting figures. This material is available free of charge via the Internet at http://pubs.acs.org.

AUTHOR INFORMATION

Corresponding Authors

runweili@nimte.ac.cn
hanlei@nbu.edu.cn
xzou@mmk.su.se

Author Contributions

[▽]L.P. and G.L. contributed equally.

Notes

The authors declare no competing financial interest.

ACKNOWLEDGMENTS

The authors thank Prof. Ren-Gen Xiong for assistance with the temperature-dependent dielectric constant measurements and Prof. Anquan Jiang, Prof. Huarong Zeng, Prof. Shibing Long, and Dr. Yi Li for fruitful discussions. The authors acknowledge financial support from the State Key Project of Fundamental Research of China (973 Program, 2012CB933004, 2009CB930803), the Chinese Academy of Sciences, the National Natural Science Foundation of China (11274321, 11474295, 21071087, 91122012, 51303194, 61328402), the Ningbo Science and Technology Innovation Team (2009B21005, 2011B82004), the Ningbo Natural Science Foundation (2013A610031), the Swedish Research Council (VR), and the Swedish Governmental Agency for Innovation Systems (VINNOVA).

REFERENCES

(1) Kwok, K. S.; Ellenbogen, J. C. *Mater. Today* **2002**, *5* (2), 28.
(2) Tao, N. J. *Nat. Nanotechnol.* **2006**, *1*, 173.
(3) Lu, W.; Lieber, C. M. *Nat. Mater.* **2007**, *6*, 841.
(4) Chang, T. C.; Jian, F. Y.; Chen, S. C.; Tsai, Y. T. *Mater. Today* **2011**, *14*, 608.
(5) Carroll, R. L.; Gorman, C. B. *Angew. Chem., Int. Ed.* **2002**, *41*, 4378.
(6) Heath, J. R.; Ratner, M. A. *Phys. Today* **2003**, *56* (5), 43.
(7) Erbe, A.; Verleger, S. *Acta Phys. Polym., A* **2009**, *115*, 455.
(8) Song, H.; Reed, M. A.; Lee, T. *Adv. Mater.* **2011**, *23*, 1583.
(9) Ratner, M. *Nat. Nanotechnol.* **2013**, *8*, 378.
(10) (a) Zhou, H.-C.; Long, J. R.; Yaghi, O. M. *Chem. Rev.* **2012**, *112*, 673. (b) Stock, N.; Biswas, S. *Chem. Rev.* **2012**, *112*, 933.
(11) (a) Sumida, K.; Rogow, D. L.; Mason, J. A.; McDonald, T. M.; Bloch, E. D.; Herm, Z. R.; Bae, T. H.; Long, J. R. *Chem. Rev.* **2012**,

112, 724. (b) Suh, M. P.; Park, H. J.; Prasad, T. K.; Lim, D. W. *Chem. Rev.* **2012**, *112*, 782. (c) Wu, H.; Gong, Q.; Olson, D. H.; Li, J. *Chem. Rev.* **2012**, *112*, 836.
(12) (a) Li, J.; Sculley, J.; Zhou, H.-C. *Chem. Rev.* **2012**, *112*, 869. (b) Kreno, L. E.; Leong, K.; Farha, O. K.; Allendorf, M.; Van Duyne, R. P.; Hupp, J. T. *Chem. Rev.* **2012**, *112*, 1105. (c) Horcajada, P.; Gref, R.; Baati, T.; Allan, P. K.; Maurin, G.; Couvreur, P.; Férey, G.; Morris, R. E.; Serre, C. *Chem. Rev.* **2012**, *112*, 1232. (d) Lee, J.; Farha, O. K.; Roberts, J.; Scheidt, K. A.; Nguyen, S. T.; Hupp, J. T. *Chem. Soc. Rev.* **2009**, *38*, 1450.
(13) (a) Wang, C.; Zhang, T.; Lin, W. *Chem. Rev.* **2012**, *112*, 1084. (b) Cui, Y. J.; Yue, Y. F.; Qian, G. D.; Chen, B. L. *Chem. Rev.* **2012**, *112*, 1126.
(14) (a) Cui, H.; Wang, Z.; Tahahashi, K.; Pkano, Y.; Kobayashi, H.; Kobayashi, A. *J. Am. Chem. Soc.* **2006**, *128*, 15074. (b) Besara, T.; Jain, P.; Dalal, N. S.; Kuhns, P. L.; Reyes, A. P.; Kroto, H. W.; Cheetham, A. K. *Proc. Natl. Acad. Sci. U.S.A.* **2011**, *108*, 6828. (c) Zhang, W.; Xiong, R. G. *Chem. Rev.* **2012**, *112*, 1163. (d) Ye, H.-Y.; Zhang, Y.; Fu, D.-W.; Xiong, R.-G. *Angew. Chem., Int. Ed.* **2014**, *53*, 6724. (e) Jain, P.; Ramachandran, V.; Clark, R. J.; Zou, H. D.; Toby, B. H.; Dalal, H. S.; Kroto, H. W.; Cheetham, A. K. *J. Am. Chem. Soc.* **2009**, *131*, 13625. (f) Stroppa, A.; Jain, P.; Barone, P.; Marsman, M.; Perezmato, J. M.; Cheetham, A. K.; Kroto, H. W.; Picozzi, S. *Angew. Chem., Int. Ed.* **2011**, *50*, 5847. (g) Sante, D. D.; Stroppa, A.; Jian, P.; Picozzi, S. *J. Am. Chem. Soc.* **2013**, *135*, 18126.
(15) (a) Kurmoo, M. *Chem. Soc. Rev.* **2009**, *38*, 1353. (b) Wriedt, M.; Yakovenko, A. A.; Halder, G. J.; Prosvirin, A. V.; Dunbar, K. R.; Zhou, H.-C. *J. Am. Chem. Soc.* **2013**, *135*, 4040.
(16) Kepert, C. J. *Chem. Commun.* **2006**, 695.
(17) Raymo, F. M. *Adv. Mater.* **2002**, *14*, 401.
(18) Liu, F.; Willhammar, T.; Wang, L.; Zhu, L.; Sun, Q.; Meng, X.; Carrillo-Cabrera, W.; Zou, X.; Xiao, F. S. *J. Am. Chem. Soc.* **2012**, *134*, 4557.
(19) Sheldrick, G. M. *Acta Crystallogr.* **2008**, *A64*, 112.
(20) Perdew, J. P.; Burke, K.; Emzerhof, M. *Phys. Rev. Lett.* **1996**, *77*, 3865.
(21) Lippert, G.; Hutter, J.; Parrinello, M. *Mol. Phys.* **1997**, *92*, 477.
(22) VandeVondele, J.; Krack, M.; Mohamed, F.; Parrinello, M.; Chassaing, T.; Hutter, J. *Comput. Phys. Commun.* **2005**, *167*, 103.
(23) Goedecker, S.; Teter, M.; Hutter, J. *Phys. Rev. B* **1996**, *54*, 1703.
(24) Hartwigsen, C.; Goedecker, S.; Hutter, J. *Phys. Rev. B* **1998**, *58*, 3641.
(25) Grimme, S. *J. Comput. Chem.* **2006**, *27*, 1787.
(26) Spek, A. L. *PLATON: A Multipurpose Crystallographic Tool*; Utrecht University: Utrecht, The Netherlands, 2003.
(27) Sun, J.; Weng, L.; Zhou, Y.; Chen, J.; Chen, Z.; Liu, Z.; Zhao, D. *Angew. Chem., Int. Ed.* **2002**, *41*, 4471.
(28) Shigematsu, A.; Yamada, T.; Kitagawa, H. *J. Am. Chem. Soc.* **2011**, *133*, 2034.
(29) Pan, C.; Nan, J.; Dong, X.; Ren, X. M.; Jin, W. *J. Am. Chem. Soc.* **2011**, *134*, 12330.
(30) Panda, T.; Kundu, T.; Banerjee, R. *Chem. Commun.* **2013**, *49*, 6197.
(31) (a) Ngai, K. L.; Rendell, R. W.; Jain, H. *Phys. Rev. B* **1984**, *30*, 2133. (b) Lee, W. K.; Liu, J. F.; Nowick, A. S. *Phys. Rev. Lett.* **1991**, *67*, 1559. (c) Lee, W. K.; Lim, B. S.; Liu, J. F.; Nowick, A. S. *Solid State Ionics* **1992**, *53*−*56*, 831. (d) Borsa, F.; Torgeson, D. R.; Martin, S. W.; Patel, H. K. *Phys. Rev. B* **1992**, *46*, 795. (e) Cutroni, N.; Mandanici, A.; Piccolo, A.; Fanggao, C.; Saunders, G. A.; Mustarelli, P. *Solid State Ionics* **1996**, *90*, 167.
(32) Valov, I. E.; Linn, S.; Tappertzhofen, S.; Schmelzer, S.; Van den Hurk, J.; Lentz, F.; Waser, R. *Nat. Commun.* **2013**, *4*, No. 1771.
(33) (a) Zhao, H. X.; Kong, X.-J.; Li, H.; Jin, Y.-C.; Long, L.-S.; Zeng, X. C.; Huang, R.-B.; Zheng, L.-S. *Proc. Natl. Acad. Sci. U.S.A.* **2011**, *108*, 3481. (b) Cui, H. B.; Zhou, B.; Long, L. S.; Okano, Y.; Kobayshi, H.; Kobayashi, A. *Angew. Chem., Int. Ed.* **2008**, *47*, 3376.
(34) Shrout, T. R. *Ultrason. Symp. Proc.* **1990**, *2*, 711.
(35) Ye, Z.-G. *Key Eng. Mater.* **1998**, *155*−*156*, 81.
(36) Hlinka, J.; Petjelt, J.; Kamba, S.; Noujni, D.; Ostapchuk, T. *Phase Transitions* **2006**, *79*, 41.
(37) Carter, R. L. *Molecular Symmetry and Group Theory*; Wiley: New York, 1998.
(38) Cotton, F. A. *Chemical Applications of Group Theory*, 3rd ed.; Wiley: New York, 1990.
(39) Sanson, M. S. P.; Biggin, P. C. *Nature* **2001**, *414*, 156.
(40) Vaidhyanathan, R.; Iremonger, S. S.; Dawson, K. W.; Shimizu, G. K. H. *Chem. Commun.* **2009**, 5230.
(41) Koga, K.; Gao, G. T.; Tanaka, H.; Zeng, X. C. *Nature* **2001**, *412*, 802.
(42) Byl, O.; Liu, J.-C.; Wang, Y.; Yim, W.-L.; Johnson, J. K.; Yates, J. T., Jr. *J. Am. Chem. Soc.* **2006**, *128*, 12090.
(43) Allendorf, M. D.; Schwartzberg, A.; Stavila, V.; Talin, A. A. *Chem.—Eur. J.* **2011**, *17*, 11372.
(44) Hendon, C. H.; Tiana, D.; Walsh, A. *Phys. Chem. Chem. Phys.* **2012**, *14*, 13120.
(45) Fu, Y.; Sun, D.; Chen, Y.; Huang, R.; Ding, Z.; Fu, X.; Li, Z. *Angew. Chem., Int. Ed.* **2012**, *124*, 3420.
(46) Son, H.; Jin, S.; Patwardhan, S.; Wezenberg, S. J.; Jeong, N. C.; So, M.; Wilmer, C. E.; Sarjeant, A. A.; Schatz, G. C.; Snurr, R. Q.; Farha, O. K.; Wiederrecht, G. P.; Hupp, J. T. *J. Am. Chem. Soc.* **2013**, *135*, 862.
(47) Burton, J. D.; Tsymbal, E. Y. *Phys. Rev. Lett.* **2011**, *106*, No. 157203.
(48) Yin, Y. W.; Burton, J. D.; Kim, Y.-M.; Borisevich, A. Y.; Pennycook, S. J.; Yang, S. M.; Noh, T. W.; Gruverman, A.; Li, X. G.; Tsymbal, E. Y.; Li, Q. *Nat. Mater.* **2013**, *12*, 397.
(49) Chen, I. *J. Appl. Phys.* **1976**, *47*, 2988.
(50) Garcia, V.; Bibes, M. *Nat. Commun.* **2014**, *5*, No. 4289.
(51) Pender, L. F.; Fleming, R. J. *J. Appl. Phys.* **1975**, *46*, 3426.
(52) Ouyang, J. Y.; Chu, C.-W.; Szmanda, C. R.; Ma, L. P.; Yang, Y. *Nat. Mater.* **2004**, *3*, 918.
(53) Donhauser, Z. J.; Montooth, B. A.; Kelly, K. F.; Bumm, L. A.; Monnell, J. D.; Stapleton, J. J.; Price, D. W.; Rawlett, A. M.; Allara, D. L.; Tour, J. M.; Weiss, P. S. *Science* **2001**, *292*, 2303.